

# Threshold Perspectives on Meson Production

M. Wolke <sup>1</sup>

*The Svedberg Laboratory, Uppsala University, Box 533, 75121 Uppsala, Sweden* \*

**Abstract.** Studies of meson production in nucleon–nucleon collisions at threshold are characterised by few degrees of freedom in a configuration of well defined initial and final states with a transition governed by short range dynamics. Effects from low–energy scattering in the exit channel are inherent to the data and probe the interaction in baryon–meson and meson–meson systems otherwise difficult to access.

From dedicated experiments at the present generation of cooler rings precise data are becoming available on differential and eventually spin observables allowing detailed comparisons between complementary final states. To discuss physics implications of generic and specific properties, recent experimental results on meson production in proton–proton scattering obtained at CELSIUS and COSY serve as a guideline.

## INTRODUCTION

High precision data from the present generation of cooler rings, IUCF, CELSIUS, and COSY, have contributed significantly over the last decade to our present knowledge and understanding of threshold meson production (for a recent review see [1]).

Due to the high momentum transfers required to create a meson or mesonic system in production experiments close to threshold the short range part of the interaction is probed. In nucleon–nucleon scattering, for mesons in the mass range up to  $1\text{ GeV}/c^2$  distances from  $0.53\text{ fm}$  ( $\pi^0$ ) down to less than  $0.2\text{ fm}$  ( $\phi$ ) are involved. At such short distances it is *a priori* not clear, whether the relevant degrees of freedom are still baryons and mesons, or rather quarks and gluons. As there is no well defined boundary, one goal of the threshold production approach is to explore the limits in momentum transfer for a consistent description using hadronic meson exchange models. Within this framework, questions concerning both the underlying meson exchange contributions and especially the role of intermediate baryon resonances have to be answered.

Another aspect which enriches the field of study arises from the low relative centre–of–mass velocities of the projectiles: Effects of low energy scattering are inherent to the observables due to strong final state interactions (FSI) within the baryon–baryon, baryon–meson, and meson–meson subsystems. In case of short–lived particles, low energy scattering potentials are otherwise difficult or impossible to study directly.

---

<sup>1</sup> email: magnus.wolke@tsl.uu.se, m.wolkel@fz-juelich.de

\* on leave from Institut für Kernphysik, Forschungszentrum Jülich, 52425 Jülich, Germany

## DYNAMICS OF THE TWO PION SYSTEM

In  $\gamma$  and  $\pi$  induced double pion production on the nucleon the excitation of the  $N^*(1440)$   $P_{11}$  resonance followed by its decay to the  $N\sigma$  channel, i.e.  $N^*(1440) \rightarrow p(\pi\pi)_{I=l=0}$ , is found to contribute non-negligibly close to threshold [2, 3, 4]. Nucleon–nucleon scattering should provide complementary information, eventually on the  $\pi\pi$  decay mode of the  $N^*(1440)$ , which plays an important part in understanding the basic structure of the second excited state of the nucleon [5, 6, 7].

Exclusive CELSIUS data from the PROMICE/WASA setup on the reactions  $pp \rightarrow pp\pi^+\pi^-$ ,  $pp \rightarrow pp\pi^0\pi^0$  and  $pp \rightarrow pn\pi^+\pi^0$  [8, 9, 10] are well described by model calculations [11]: For the  $\pi^+\pi^-$  and  $\pi^0\pi^0$  channels, the reaction preferentially proceeds close to threshold via heavy meson exchange and excitation of the  $N^*(1440)$  Roper resonance, with a subsequent pure s-wave decay to the  $N\sigma$  channel<sup>1</sup>. While nonresonant contributions are expected to be small, resonant processes with Roper excitation and decay via an intermediate  $\Delta$  ( $pp \rightarrow pN^* \rightarrow p\Delta\pi \rightarrow pp\pi\pi$ ) and  $\Delta\Delta$  excitation ( $pp \rightarrow \Delta\Delta \rightarrow p\pi p\pi$ ) are strongly momentum dependent and vanish directly at threshold. Double  $\Delta$  excitation, which is expected to dominate at higher excess energies beyond  $Q = 250$  MeV [11] involves higher angular momenta and consequently strongly anisotropic proton and pion angular distributions. On the other hand, the Roper decay amplitude via an intermediate  $\Delta$  depends predominantly on a term symmetric in the pion momenta (eq.(1)), leading to the  $p(\pi^+\pi^-)_{I=l=0}$  channel and an interference with the direct  $N\sigma$  decay.

Experimentally, for the reaction  $pp \rightarrow pp\pi^+\pi^-$  at excess energies of  $Q = 64.4$  MeV and  $Q = 75$  MeV angular distributions give evidence for only s-waves in the final state, in line with a dominating  $pp \rightarrow pN^* \rightarrow pp(\pi^+\pi^-)_{I=l=0}$  process, with the initial inelastic  $pp$  collision governed by heavy meson ( $\sigma, \rho$ ) exchange. Roper excitation is disclosed in the  $p\pi^+\pi^-$  invariant mass distribution (Fig.1a), where the data are shifted towards higher invariant masses compared to phase space in agreement with resonance excitation in the low energy tail of the  $N^*(1440)$ . Compared with Monte Carlo simulations including both heavy meson exchange for  $N^*$  excitation, and  $pp$  S-wave final state interaction, but only the direct decay  $N^* \rightarrow p(\pi^+\pi^-)_{I=l=0}$  (dotted lines), the production process involves additional dynamics, which is apparent from discrepancies especially in observables depending on the  $\pi$  momentum correlation  $\vec{k}_1 \cdot \vec{k}_2$ , i.e.  $\pi^+\pi^-$  invariant mass  $M_{\pi\pi}$  (Fig.1b) and opening angle  $\delta_{\pi\pi} = \angle(\vec{k}_1 \cdot \vec{k}_2)$  (Fig.1c). A good description of the experimental data is achieved including the  $N^*(1440)$  decay via an intermediate  $\Delta$  and its destructive interference with the direct decay branch to the  $N\sigma$  channel (solid lines) in the ansatz for the Roper decay amplitude [11]:

$$\mathcal{A} \propto 1 + c \vec{k}_1 \cdot \vec{k}_2 (3D_{\Delta^{++}} + D_{\Delta^0}), \quad (1)$$

where the first term describes the direct decay, the parameter  $c$  adjusts the relative strengths of the two decay routes, and  $D_\Delta$  denote the  $\Delta$  propagators. A fit to the data

---

<sup>1</sup> For the  $pn\pi^+\pi^0$  final state, this reaction mechanism is trivially forbidden by isospin conservation. An underestimation of the total cross section data [9] by the model predictions [11] might be explained by the neglect of effects from the  $pn$  final state interaction in the calculation [12].

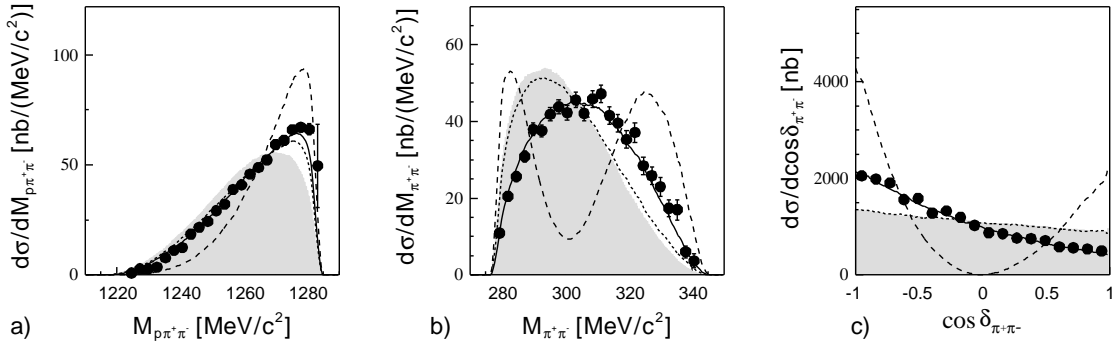


**FIGURE 1.** Differential cross sections for the reaction  $pp \rightarrow pp\pi^+\pi^-$  at an excess energy of  $Q = 75$  MeV. Experimental data (solid circles) for invariant mass distributions of the  $(p\pi^+\pi^-)$ - (a) and  $(\pi^+\pi^-)$ -subsystems (b), and the  $\pi^+\pi^-$  opening angle (c) are compared to pure phase space (shaded areas) and Monte Carlo simulations for direct decays  $N^* \rightarrow N\sigma$  (dotted lines), decays via an intermediate  $\Delta$  resonance  $N^* \rightarrow \Delta\pi \rightarrow N\sigma$  (dashed lines) and an interference of the two decay routes (solid lines) according to eq.(1). Figures are taken from [10].

allows to determine the ratio of partial decay widths  $\mathcal{R}(M_{N^*}) = \Gamma_{N^* \rightarrow \Delta\pi \rightarrow N\pi\pi} / \Gamma_{N^* \rightarrow N\sigma}$  at average masses  $\langle M_{N^*} \rangle$  corresponding to excess energies  $Q = 64.4$  MeV and  $Q = 75$  MeV relative to the  $\pi^+\pi^-$  threshold. The numerical results,  $\mathcal{R}(1264) = 0.034 \pm 0.004$  and  $\mathcal{R}(1272) = 0.054 \pm 0.006$ , exhibit the clear dominance of the direct decay to the  $N\sigma$  channel in the low energy region of the Roper resonance. On the other hand they indicate the strong energy dependence of the ratio from the momentum dependence in the decay branch via an intermediate  $\Delta$ , which will surpass the direct decay at higher energies [10]. A model dependent extrapolation based on the validity of ansatz (1) leads to  $\mathcal{R}(1440) = 3.9 \pm 0.3$  at the nominal resonance pole in good agreement with the PDG value of  $4 \pm 2$  [13].

Within the experimental programme to determine the energy dependence of the  $N^* \rightarrow N\pi\pi$  decay exclusive data (for details see [14]) have been taken simultaneously at the CELSIUS/WASA facility on both the  $pp\pi^+\pi^-$  and  $pp\pi^0\pi^0$  final states. In case of the  $\pi^+\pi^-$  system the preliminary results at an excess energy of  $Q = 75$  MeV are in good agreement with the relative strength of the decay routes adjusted to an extrapolated ratio  $\mathcal{R}(1440) = 3$ . However, at slightly higher excess energy ( $Q = 127$  MeV) the data might be equally well described by a value  $\mathcal{R}(1440) = 1$ , which is noticeably favoured at both excess energies by the data on  $\pi^0\pi^0$  production, indicating distinct underlying dynamics in  $\pi^0\pi^0$  and  $\pi^+\pi^-$  production. One difference becomes obvious from the isospin decomposition of the total cross section [9]: An isospin  $I = 1$  amplitude in the  $\pi\pi$  system, and accordingly a p-wave admixture, is forbidden by symmetry to contribute to the neutral pion system in contrast to the charged complement. A p-wave component was neglected so far in the analysis, since the unpolarized angular distributions show no deviation from isotropy. However, there is evidence for small, but non-negligible analysing powers from a first exclusive measurement of  $\pi^+\pi^-$  production with a polarized beam at the COSY-TOF facility [14, 15], suggesting higher partial waves especially in the  $\pi\pi$  system.

At higher energies, i.e.  $Q = 208$  MeV and  $Q = 286$  MeV with respect to the  $\pi^+\pi^-$

threshold, preliminary data for both  $\pi^+\pi^-$  and  $\pi^0\pi^0$  from CELSIUS/WASA rather follow phase space than expectations based on a dominating  $pp \rightarrow pN^* \rightarrow pp\sigma$  reaction mechanism[14]. At these energies, the  $\Delta\Delta$  excitation process should influence observables significantly, and, thus, a phase space behaviour becomes even more surprising, unless the  $\Delta\Delta$  system is excited in a correlated way.

## THE PROTON-PROTON-ETA FINAL STATE

As a general trait in meson production in nucleon-nucleon scattering, the primary production amplitude, i. e. the underlying dynamics can be regarded as energy independent in the vicinity of threshold [16, 17, 18]. Consequently, for s-wave production processes, the energy dependence of the total cross section is essentially given by a phase space behaviour modified by the influence of final state interactions. In Fig.2 total cross section data obtained in proton-proton scattering are shown for the pseudoscalar isosinglet mesons  $\eta$  and  $\eta'$  [19]. In both cases, the energy dependence of the total cross sec-

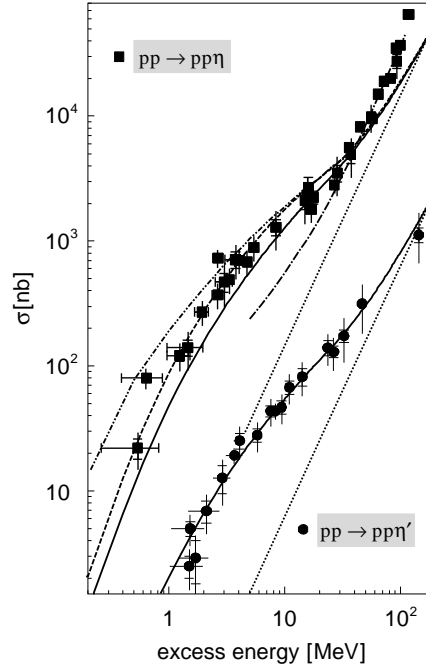


**FIGURE 2.** Total cross section data for  $\eta$  (squares [20, 21, 22, 23, 24, 25]) and  $\eta'$  (circles [24, 26, 27, 28, 29]) production in proton-proton scattering versus excess energy  $Q$  [19]. In comparison, the energy dependences from a pure phase space behaviour (dotted lines, normalized arbitrarily), from phase space modified by the  $^1S_0$  proton-proton FSI including Coulomb interaction (solid lines), and from additionally including the proton- $\eta$  interaction phenomenologically (dashed line), are shown. Meson exchange calculations for  $\eta$  production including a P-wave component in the proton-proton system [30] are depicted by the dashed-dotted line, while the dashed-double-dotted line corresponds to the arbitrarily normalized energy dependence from a full three-body treatment of the  $pp\eta$  final state [31] (see also [32]).

tion deviates significantly from phase space expectations. Including the on-shell  $^1S_0$  proton-proton FSI enhances the cross section close to threshold by more than an order of magnitude, in good agreement with data in case of  $\eta'$ . As expected from kinemat-

ical considerations [1] the cross section for  $\eta$  production deviates from phase space including the  $pp$  FSI at excess energies  $Q \geq 40\text{ MeV}$ , where the  $^1\text{S}_0$  final state is no longer dominant compared to higher partial waves. Deviations at low excess energies seem to be well accounted for by an attractive proton– $\eta$  FSI (dashed line), treated phenomenologically as an incoherent pairwise interaction [1, 17, 33]. In comparison to the proton– $\eta'$  (Fig.2) and proton– $\pi^0$  systems only the  $p\eta$  interaction is strong enough to become apparent in the energy dependence of the total cross section [34]. In differential observables, effects should be more pronounced in the phase space region of low proton– $\eta$  invariant masses. However, to discern effects of proton– $\eta$  scattering from the influence of proton–proton FSI, which is stronger by two orders of magnitude, requires high statistics measurements, which have only become available recently [19, 35, 36]: Close to threshold, the distribution of the invariant mass of the proton–proton subsys-

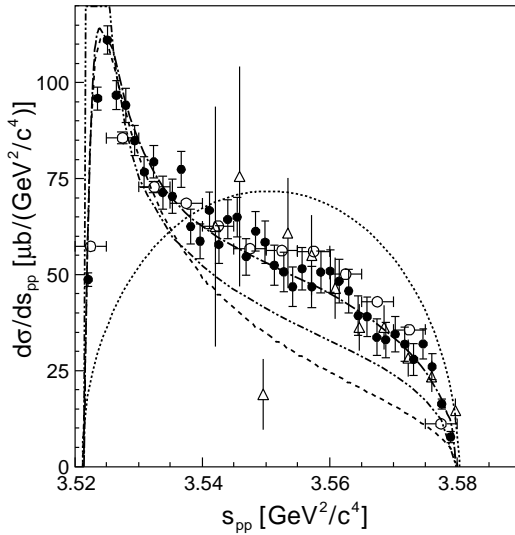


**FIGURE 3.** Invariant mass squared of the  $(pp)$ -subsystem in the reaction  $pp \rightarrow pp\eta$  at excess energies of  $Q = 15.5\text{ MeV}$  (COSY-11, solid circles [19]),  $Q = 15\text{ MeV}$  (COSY-TOF, open circles [36]) and  $Q = 16\text{ MeV}$  (PROMICE/WASA, open triangles [35]). The dotted and dashed lines follow a pure phase space behaviour and its modification by the phenomenological treatment of the three–body FSI as an incoherent pairwise interaction, respectively. The latter was normalized at small invariant mass values. Effects from including a P–wave admixture in the  $pp$  system are depicted by the dashed–dotted line [30], while the dashed–double–dotted line corresponds to a pure s–wave final state with a full three–body treatment [32].

tem is characteristically shifted towards low invariant masses compared to phase space (dotted line in Fig.3). This low–energy enhancement is well reproduced by modifying phase space with the  $^1\text{S}_0$   $pp$  on–shell interaction. A second enhancement at higher  $pp$  invariant masses, i.e. low energy in the  $p\eta$  system, is not accounted for even when including additionally the proton– $\eta$  interaction incoherently (dashed line). However, including a P–wave admixture in the  $pp$  system by considering a  $^1\text{S}_0 \rightarrow ^3\text{P}_0s$  transition in addition to the  $^3\text{P}_0 \rightarrow ^1\text{S}_0s$  threshold amplitude, excellent agreement with the experimental invariant mass distribution is obtained (dashed–dotted line [30]). In return, with the P–wave strength adjusted to fit the invariant mass data, the approach fails to reproduce the energy dependence of the total cross section (Fig.2) below excess energies of  $Q = 40\text{ MeV}$ . Preliminary calculations considering only s–waves in the final state

but using a rigorous three–body treatment of the  $pp\eta$  final state actually decrease the cross section at large values of the  $pp$  invariant mass (dashed–double–dotted lines [32]) compared to an incoherent two–body calculation within the same framework. However, close to threshold the energy dependence of the total cross section is enhanced compared to the phenomenological incoherent treatment and the data (Fig.2). Although part of this enhancement has to be attributed to the neglect of Coulomb repulsion in the  $pp$  system, consequently overestimating the  $pp$  invariant mass at low values, qualitatively the full three–body treatment has opposite effects compared to a P–wave admixture in the proton–proton system in view of both the total cross section as well as the  $pp$  invariant mass distribution. In the approximate description of the total cross section by the phenomenological s–wave approach with an incoherent FSI treatment these two effects seem to cancel casually.

Close to threshold, resonance excitation of the  $S_{11}(1535)$  and subsequent decay to the  $p\eta$  final state is generally<sup>2</sup> believed to be the dominant  $\eta$  production mechanism [17, 30, 38, 39, 40, 41, 42, 43]. In this context, the issue of the actual excitation mechanism of the  $S_{11}(1535)$  remains to be addressed. The  $\eta$  angular distribution is sensitive to the underlying dynamics: A dominant  $\rho$  exchange favoured in [41] results in an inverted curvature of the  $\eta$  angular distribution compared to  $\pi$  and  $\eta$  exchanges which are inferred to give the largest contribution to resonance excitation in [42]. In the latter approach the interference of the pseudoscalar exchanges in the resonance current with non–resonant nucleonic and mesonic exchange currents turns the curvature to the same angular dependence as expected for  $\rho$  exchange. Presently, due to the statistical errors of the available unpolarised data at an excess energy of  $Q \approx 40$  MeV [35, 36] it is not possible to differentiate between a dominant  $\rho$  or  $\pi$ ,  $\eta$  exchange, as discussed in [36]. Data recently taken at the CELSIUS/WASA facility with statistics increased by an order of magnitude compared to the available data might provide an answer in the near future [44].

Spin observables, like the  $\eta$  analyzing power, should even disentangle a dominant  $\rho$  meson exchange and the interference of  $\pi$  and  $\eta$  exchanges in resonance excitation with small nucleonic and mesonic currents [42], which result in identical predictions for the unpolarised  $\eta$  angular distribution. First data [45] seem to favour the vector dominance model, but final conclusions both on the underlying reaction dynamics and the admixture of higher partial waves [30] have to await the analysis of data taken with higher statistics for the energy dependence of the  $\eta$  analysing power [46].

## ASSOCIATED STRANGENESS PRODUCTION

In elementary hadronic interactions with no strange valence quark in the initial state the associated strangeness production provides a powerful tool to study reaction dynamics

---

<sup>2</sup> The  $pn \rightarrow d\eta$  excitation function has been interpreted to provide direct experimental evidence for  $S_{11}(1535)$  excitation [23]. It should be noted, however, that in [37] for  $\eta$  production in proton–proton scattering short range nucleonic currents, i.e.  $\sigma$  and  $\omega$  exchange are found to be much stronger compared to the contribution from resonance currents.

by introducing a “tracer” to hadronic matter. Thus, quark model concepts might eventually be related to mesonic or baryonic degrees of freedom, with the onset of quark degrees of freedom expected for kinematical situations with large enough transverse momentum transfer.

First exclusive close-to-threshold data on  $\Lambda$  and  $\Sigma^0$  production [47, 48] obtained at the COSY-11 facility showed at equal excess energies below  $Q = 13\text{ MeV}$  a cross section ratio of

$$\mathcal{R}_{\Lambda/\Sigma^0}(Q \leq 13\text{ MeV}) = \frac{\sigma(pp \rightarrow pK^+\Lambda)}{\sigma(pp \rightarrow pK^+\Sigma^0)} = 28^{+6}_{-9} \quad (2)$$

exceeding the high energy value ( $Q \geq 300\text{ MeV}$ ) of 2.5 [49] by an order of magnitude.

In the meson exchange framework, estimates for  $\pi$  and  $K$  exchange contributions based on the elementary scattering processes do not reproduce the experimental value (2) [48, 50]. However, inclusive  $K^+$  production data in  $pp$  scattering at an excess energy of  $Q = 252\text{ MeV}$  with respect to the  $pK^+\Lambda$  threshold show enhancements at the  $\Lambda p$  and  $\Sigma N$  thresholds of similar magnitude [51]. Qualitatively, a strong  $\Sigma^0 N \rightarrow \Lambda p$  final state conversion might account for both the inclusive SATURNE results as well as the  $\Sigma^0$  depletion in the COSY-11 data. Evidence for such conversion effects is known e. g. from fully constrained kaon absorption on deuterium via  $K^- d \rightarrow \pi^- \Lambda p$  [52].

In exploratory calculations performed within the framework of the Jülich meson exchange model [50], taking into account both  $\pi$  and  $K$  exchange diagrams in a coupled channel approach, a final state conversion is rather excluded as origin of the experimentally observed ratio: While  $\Lambda$  production is found to be dominated by kaon exchange, both  $\pi$  and  $K$  exchange turn out to contribute to the  $\Sigma^0$  channel with similar strength. Qualitatively, this result is experimentally confirmed at higher excess energies between  $Q = 200\text{ MeV}$  and  $Q = 430\text{ MeV}$  from polarization transfer measurements from the DISTO experiment [53, 54, 55]. It is concluded in [50], that only a destructive interference of  $\pi$  and  $K$  exchange might explain the experimental value (2).  $\Sigma$  production in different isospin configurations should provide a crucial test for this interpretation, since for the reaction  $pp \rightarrow nK^+\Sigma^+$  the interference pattern is found to be opposite compared to the  $pK^+\Sigma^0$  channel. Data close to threshold have recently been taken at the COSY-11 facility [56].

However, within an effective Lagrangian approach [57] both  $\Lambda$  and  $\Sigma^0$  production channels are concluded to be dominated by  $\pi$  exchange and excitation of the  $S_{11}(1650)$  close to threshold, while at excess energies above  $Q = 300\text{ MeV}$  the  $N^*(1710)$  governs strangeness production<sup>3</sup>. In this energy range the influence of resonances becomes evident from recent data on invariant mass distribution determined at COSY-TOF [59].

To study the transition region between the low-energy enhancement (2) and the high energy value measurements have been extended up to excess energies of  $Q = 60\text{ MeV}$  [58, 60]: In order to describe the energy dependence of the total cross section for  $\Lambda$  production, in addition to phase space the  $p\Lambda$  final state interaction has to be taken into account. In contrast,  $\Sigma^0$  production is satisfactorily well described by phase space behaviour only [58]. This qualitatively different behaviour might be explained by the

---

<sup>3</sup> For further complementary theoretical approaches see references in [1, 58, 59].

$\Sigma^0 p$  FSI being much weaker compared to the  $\Lambda p$  system. However, the interpretation implies dominant S-wave production and reaction dynamics that can be regarded as energy independent. Within the present level of statistics, contributions from higher partial waves can be neither ruled out nor confirmed at higher excess energies for  $\Sigma^0$  production.

The energy dependence of the production ratio  $\mathcal{R}_{\Lambda/\Sigma^0}$  is shown in Fig.4 in comparison with theoretical calculations obtained within the approach of [50] assuming a destructive interference of  $\pi$  and  $K$  exchange and employing different choices of the microscopic hyperon nucleon model to describe the interaction in the final state [61]. The result

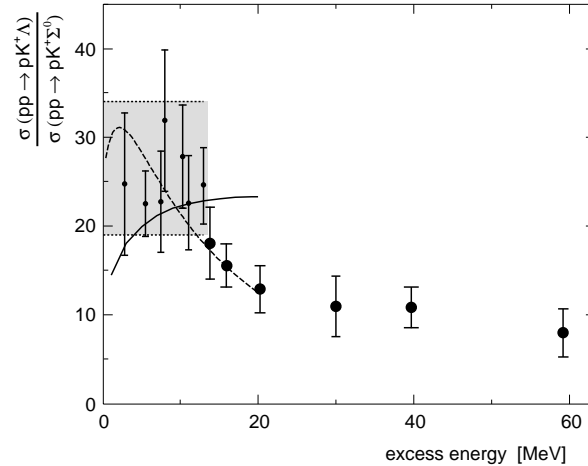


**FIGURE 4.**  $\Lambda/\Sigma^0$  production ratio in proton–proton scattering as a function of the excess energy. Data are from [48] (shaded area) and [60]. Calculations [61] within the Jülich meson exchange model imply a destructive interference of  $K$  and  $\pi$  exchange using the microscopic Nijmegen NSC89 (dashed line [62]) and the new Jülich model (solid line [63]) for the  $YN$  final state interaction.

crucially depends on the details — especially the off–shell properties — of the hyperon–nucleon interaction employed. At the present stage both the good agreement found in [50] with the threshold enhancement (2) and for the Nijmegen model (dashed line in Fig.4) with the energy dependence of the cross section ratio should rather be regarded as accidental<sup>4</sup>. Calculations using the new Jülich model (solid line in Fig.4) do not reproduce the tendency of the experimental data. It is suggested in [61] that neglecting the energy dependence of the elementary amplitudes and higher partial waves might no longer be justified beyond excess energies of  $Q = 20$  MeV. However, once the reaction mechanism for close–to–threshold hyperon production is understood, exclusive data should provide a strong constraint on the details of hyperon–nucleon interaction models.

<sup>4</sup> In the latter case an SU(2) breaking in the  $^3S_1$   $\Sigma N$  channel had to be introduced [62] resulting in an ambiguity for the  $\Sigma^0 p$  amplitude.

## PRESENT AND FUTURE

Intermediate baryon resonances emerge as a common feature in the dynamics of the exemplary cases for threshold meson production in nucleon–nucleon scattering discussed in this article. However, this does not hold in general for meson production in the  $1\text{ GeV}/c^2$  mass range (for a discussion on  $\eta'$  production see [64]). Moreover, the extent to which resonances are evident in the observables or actually govern the reaction mechanism depends on the specific channels, which differ in view of the level of present experimental and theoretical understanding.

The  $N^*(1440)$  resonance dominates  $\pi^+\pi^-$  production at threshold, and exclusive data allow to extract resonance decay properties in the low–energy tail of the Roper. Dynamical differences between the different isospin configurations of the  $\pi\pi$  system and the behaviour at higher energies remains to be understood with first experimental clues appearing.

With three strongly interacting particles in the final state, a consistent description of  $\eta$  production close to threshold requires an accurate three–body approach taking into account the possible influence of higher partial waves. High statistics differential cross sections and polarization observables coming up should straighten out both the excitation mechanism of the  $N^*(1535)$  and the admixture of higher partial waves.

At present, the available experimental data on the elementary strangeness production channels give evidence for both an important role of resonances coupling to the hyperon–kaon channels and on a dominant non–resonant kaon exchange mechanism. Experiments on different isospin configurations, high statistics and spin transfer measurements close to threshold should disentangle the situation in future.

From the cornerstone of total cross section measurements, it is apparent from the above examples to what extent our knowledge is presently enlarged by differential observables and what will be the impact of polarization experiments in future to get new perspectives in threshold meson production.

## ACKNOWLEDGMENTS

The author gratefully acknowledges the pleasure to work with the CELSIUS/WASA and COSY–11 collaborations, and, in particular, thanks M. Bashkanov, H. Clement, R. Meier, P. Moskal and W. Oelert for helpful discussions . This work has been supported by The Swedish Foundation for International Cooperation in Research and Higher Education (STINT Kontrakt Dnr 02/192).

## REFERENCES

1. Moskal, P., Wolke, M., Khoukaz, A., and Oelert, W., *Prog. Part. Nucl. Phys.*, **49**, 1–90 (2002).
2. Oset, E., and Vicente-Vacas, M. J., *Nucl. Phys.*, **A 446**, 584–612 (1985).
3. Bernard, V., Kaiser, N., and Meißner, U.-G., *Nucl. Phys.*, **B 457**, 147–174 (1995).
4. Gómez Tejedor, J. A., and Oset, E., *Nucl. Phys.*, **A 600**, 413–435 (1996).
5. Morsch, H. P., and Zupranski, P., *Phys. Rev.*, **C 61**, 024002 (2000).

6. Krehl, O., Hanhart, C., Krewald, S., and Speth, J., *Phys. Rev.*, **C 62**, 025207 (2000).
7. Hernández, E., Oset, E., and Vicente Vacas, M. J., *Phys. Rev.*, **C 66**, 065201 (2002).
8. Brodowski, W., et al., *Phys. Rev. Lett.*, **88**, 192301 (2002).
9. Johanson, J., et al., *Nucl. Phys.*, **A 712**, 75–94 (2002).
10. Pätzold, J., et al., *Phys. Rev.*, **C 67**, 052202 (2003).
11. Alvarez-Ruso, L., Oset, E., and Hernández, E., *Nucl. Phys.*, **A 633**, 519–546 (1998).
12. Alvarez-Ruso, L. (2002), private communications.
13. Hagiwara, K., et al., *Phys. Rev.*, **D 66**, 010001 (2002).
14. Bashkanov, M., et al., proceedings of this conference (2003).
15. Clement, H., et al., Annual Report 2002, Forschungszentrum Jülich (2003), JüL-4052.
16. Moalem, A., Gedalin, E., Razdolskaja, L., and Shorer, Z., *Nucl. Phys.*, **A 600**, 445–460 (1996).
17. Bernard, V., Kaiser, N., and Meißner, U.-G., *Eur. Phys. J.*, **A 4**, 259–275 (1999).
18. Gedalin, E., Moalem, A., and Razdolskaja, L., *Nucl. Phys.*, **A 650**, 471–482 (1999).
19. Moskal, P., et al., e-Print Archive: nucl-ex/0307005 (2003), *Phys. Rev. C*, in print.
20. Bergdolt, A. M., et al., *Phys. Rev.*, **D 48**, 2969–2973 (1993).
21. Chiavassa, E., et al., *Phys. Lett.*, **B 322**, 270–274 (1994).
22. Calén, H., et al., *Phys. Lett.*, **B 366**, 39–43 (1996).
23. Calén, H., et al., *Phys. Rev. Lett.*, **79**, 2642–2645 (1997).
24. Hibou, F., et al., *Phys. Lett.*, **B 438**, 41–46 (1998).
25. Smyrski, J., Wüstner, P., et al., *Phys. Lett.*, **B 474**, 182–187 (2000).
26. Moskal, P., et al., *Phys. Rev. Lett.*, **80**, 3202–3205 (1998).
27. Moskal, P., et al., *Phys. Lett.*, **B 474**, 416–422 (2000).
28. Balestra, F., et al., *Phys. Lett.*, **B 491**, 29–35 (2000).
29. Khoukaz, A., et al., Annual report 2000/01, Institute of Nuclear Physics, University of Münster (2001), URL <http://www.uni-muenster.de/Physik/KP/anrep>.
30. Nakayama, K., Haidenbauer, J., Hanhart, C., and Speth, J., *Phys. Rev.*, **C 68**, 045201 (2003).
31. Fix, A. (2003), private communications.
32. Fix, A., and Arenhövel, H., *Nucl. Phys.*, **A 697**, 277–302 (2002).
33. Schuberth, U., Phd thesis, Uppsala University (1995).
34. Moskal, P., et al., *Phys. Lett.*, **B 482**, 356–362 (2000), and references therein.
35. Calén, H., et al., *Phys. Lett.*, **B 458**, 190–196 (1999).
36. Abdel-Bary, M., et al., *Eur. Phys. J.*, **A 16**, 127–137 (2003).
37. Peña, M. T., Garcilazo, H., and Riska, D. O., *Nucl. Phys.*, **A 683**, 322–338 (2001).
38. Batinić, M., Švarc, A., and Lee, T.-S. H., *Phys. Scripta*, **56**, 321–324 (1997).
39. Santra, A. B., and Jain, B. K., *Nucl. Phys.*, **A 634**, 309–324 (1998).
40. Gedalin, E., Moalem, A., and Razdolskaja, L., *Nucl. Phys.*, **A 634**, 368–392 (1998).
41. Fäldt, G., and Wilkin, C., *Phys. Scripta*, **64**, 427–438 (2001).
42. Nakayama, K., Speth, J., and Lee, T.-S. H., *Phys. Rev.*, **C 65**, 045210 (2002).
43. Baru, V., et al., *Phys. Rev.*, **C 67**, 024002 (2003).
44. Złomanczuk, J. (2003), private communications.
45. Winter, P., et al., *Phys. Lett.*, **B 544**, 251–258 (2002).
46. Czyżkiewicz, R., et al., proceedings of this conference (2003).
47. Balewski, J. T., et al., *Phys. Lett.*, **B 420**, 211–216 (1998).
48. Sewerin, S., Schepers, G., et al., *Phys. Rev. Lett.*, **83**, 682–685 (1999).
49. Baldini, A., Flaminio, V., Moorhead, W. G., and Morrison, D. R. O., *Total Cross-Sections for Reactions of High-Energy Particles*, vol. 12 B of *Landolt-Börnstein: New Series. Group 1*, edited by H. Schopper, Springer, Heidelberg, Germany, 1988, ISBN 3-540-18412-0.
50. Gasparian, A., et al., *Phys. Lett.*, **B 480**, 273–279 (2000).
51. Siebert, R., et al., *Nucl. Phys.*, **A 567**, 819–843 (1994).
52. Tan, T. H., *Phys. Rev. Lett.*, **23**, 395–398 (1969).
53. Balestra, F., et al., *Phys. Rev. Lett.*, **83**, 1534–1537 (1999).
54. Maggiora, M., *πN Newslett.*, **16**, 273–279 (2002).
55. Laget, J. M., *Phys. Lett.*, **B 259**, 24–28 (1991).
56. Rożek, T., and Grzonka, D., COSY Proposal 117, IKP, FZ Jülich, Germany (2002), URL <http://www.fz-juelich.de/ikp/en/publications.shtml>.
57. Shyam, R., Penner, G., and Mosel, U., *Phys. Rev.*, **C 63**, 022202 (2001).

58. Kowina, P., et al., proceedings of this conference (2003).
59. Wagner, M., et al., proceedings of this conference (2003).
60. Kowina, P., Wolke, M., et al., e-Print Archive: nucl-ex/0302014 (2003).
61. Gasparyan, A., *Symposium on Threshold Meson Production in pp and pd Interaction*, Forschungszentrum Jülich, Germany, 2002, vol. 11 of *Matter and Material*, pp. 205–211.
62. Maessen, P. M. M., Rijken, T. A., and de Swart, J. J., *Phys. Rev.*, **C 40**, 2226–2245 (1989).
63. Haidenbauer, J., Melnitchouk, W., and Speth, J., *AIP Conf. Proc.*, **603**, 421–424 (2001).
64. Moskal, P., et al., proceedings of this conference (2003).